Simulation Studies of Shallow Convection with the Convection-Resolving Version of the DWD Lokal-Modell

F. Theunert[1], A. Seifert[2]

[1] *Amt für Geo-Informationswesen der Bundeswehr, Traben-Trarbach, Germany*
[2] *Deutscher Wetterdienst, Offenbach, Germany*

1 Introduction

The next generation of mesoscale NWP models will - at least to some extent - resolve deep convection, e.g. squall lines. Most of the modeling systems currently under development aim at a grid resolution of 2-4 km. At DWD the first convection-resolving version of LM, called Lokal-Modell-Kürzestfrist[2] (LMK), will have a horizontal resolution of approximately 2.8 km. Other examples of convection-resolving NWP models are the WRF model, which was successfully applied at 4 km resolution to resolve squall lines and mesoscale convective systems in the continental U.S., the AROME project of MeteoFrance and the high-resolution version of the UK MetOffice Unified Model.

Although all these models may describe deep moist convection explicitly by the model equation system, shallow convection can currently only be considered as a sub-scale process. Therefore the important impact of shallow convection on the vertical transport of energy and water vapor has to be included by applying a special parameterization scheme. For LMK a simple shallow convection scheme based on the cumulus parameterization of Tiedtke (1989) was suggested by Doms and Förstner (2004).

In the following we will give an overview of the Tiedtke-Doms shallow convection scheme, present some case studies and verification as well as some ideas for potential improvements.

2 The Tiedtke-Doms shallow convection scheme

The Tiedtke scheme, which is operationally applied in the 7 km version of LM to parameterize cumulus convection, distinguishes between 3 cloud types: deep convection, mid-level convection and shallow convection. It is therefore rather straightforward to reduce the scheme to shallow convection only as suggested by Doms and Förstner (2004). Here we will just summarize the basic assumptions of this approach:

1. The momentum fluxes are neglected, only temperature and moisture are affected directly by shallow convection.
2. Shallow convection is non-precipitating, i.e. rain formation is neglected completely and no evaporation of rain below cloud base occurs.
3. Shallow convection does not induce convective downdrafts.
4. The moisture convergence mass flux closure is applied (Eq. 19 of Tiedtke, 1989)
5. Organized entrainment is neglected. For turbulent entrainment/detrainment $\epsilon_u = \delta_u = 3 \times 10^{-4}\ \mathrm{m}^{-1}$ is used as in Tiedtke (1989).

[2] Kürzestfrist (German) = shortest-range

a) without shallow conv. scheme b) with shallow conv. scheme

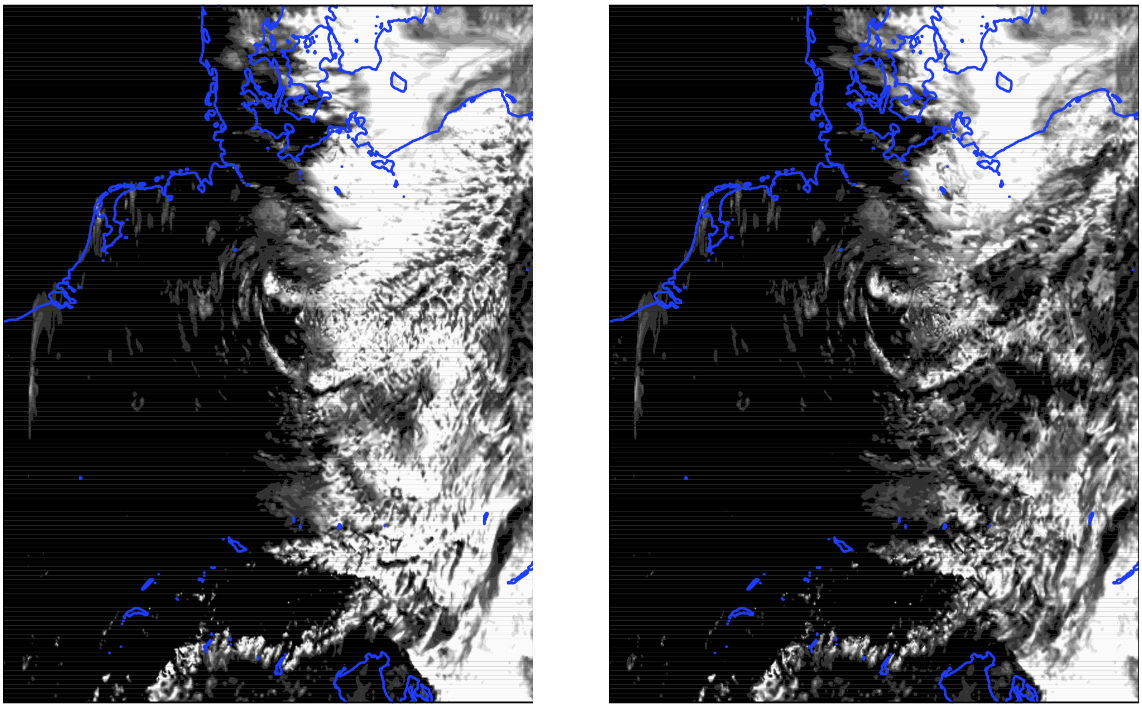

Figure 1: Simulated low-level cloud cover 29.05.2004 at 12 UTC in units of 1/8

6. Exactly the same triggering and parcel ascent calculation is used as in the full Tiedtke scheme. As in the operational Tiedtke scheme of LM horizontally averaged values of the vertical velocity and the moisture convergence are used.

7. Shallow convection is limited to a cloud depth of 250 hPa. For deeper clouds the scheme is simply turned off.

The last assumption replaces the moisture convergence threshold which distinguishes shallow convection from deep convection in the original Tiedtke scheme.

The scheme is implemented in LM 3.16 and can be turned on by setting `lconv=.true.`, `ltiedtke=.false.`, `lshallow=.true.`.

3 Case study 29 May 2004

This was a typical summertime high-pressure situation with a surface high centered over northern Germany. During daytime shallow convection developed especially over eastern Germany. This day was chosen to be able to use measurements of the Lindenberg observatory located about 100 km southeast of Berlin.

Fig. 1 shows the low-level cloud cover at 12 UTC. Compared to the 27 Feb. 2004 case shown by Doms and Förstner (2004), the reduction in cloud cover due to the shallow convection scheme is weaker, but still significant. In the simulation without shallow convection scheme the model tries to represent the cloud-topped convective boundary layer explicitly leading to an overestimation of cloud cover (note that grid-scale clouds are always counted as 100% cloud cover). Using the shallow convection scheme, the small cumuli are described as being of sub-grid scale and the associated cloud cover is drastically reduced. This can lead to a significant change in the radiation budget and the 2m-temperature. Without the shallow

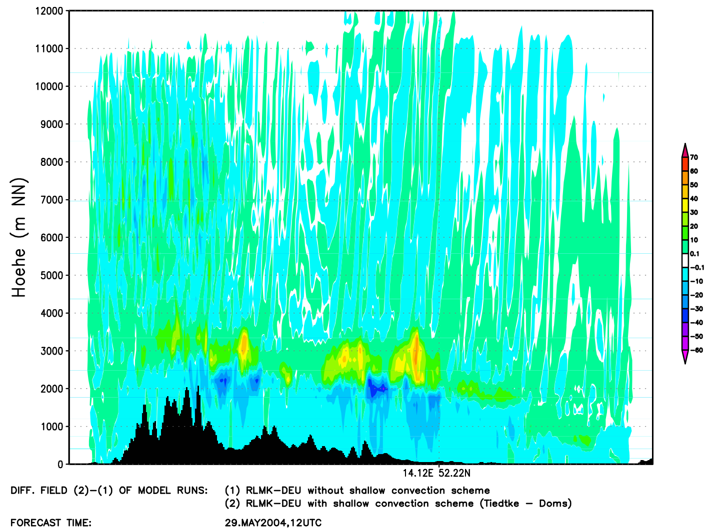

Figure 2: Vertical cross section of the difference in rel. humidity with and without shallow conv. scheme, RH_{with} - $RH_{w/o}$, in %. The cross section is oriented South-North at 14.12^{o}E.

convection parameterization the model has also deficiencies in representing the moisture fluxes due to the vertical motions within the convective boundary layer. Fig. 2 shows a vertical cross section of the difference in relative humidity between the simulation with and without shallow convection scheme. Obviously, the parameterization provides an efficient vertical transport of moisture out of the boundary layer. The rel. humidity in the PBL is reduced by about 10 % or more and the moisture is detrained in the free atmosphere. A more detailed evaluation of this process is possible by comparison with measured vertical profiles at the Lindenberg observatory located at 14.12^{o}E 52.22^{o}N.

Fig. 3 shows profiles of temperature, rel. humidity and water vapor mixing ratio for 12 UTC and 18 UTC. While the temperature profiles of both simulations matches the observations very well including the location of the PBL height, the rel. humidity and vapor mixing ratio within the PBL are overestimated, especially by the simulation without shallow convection scheme. Applying the Tiedtke-Doms scheme results in a significant reduction of the rel. humidity with the maximum being reduced from 100 %, i.e. grid-scale cloud, to 85 %. Although the rel. hum. within the PBL is still overestimated, as is the vapor mixing ratio, this seems to be an improvement compared to the simulation without shallow convection scheme. The moisture is deposited above the PBL in a layer between 2-4 km AGL making this layer much moister than observed in this case. For 18 UTC the observations show an increase in temperature and PBL height as well as a decrease of the moisture within the PBL compared to 12 UTC, both features are not reproduced by either one of the simulations. Obviously the model has some deficiencies here which may be related to treatment of soil moisture or the turbulence scheme. Since these problems are larger than the impact of the shallow convection scheme, the question arises whether the improvement by using the shallow convection scheme, also at 12 UTC, is maybe due to wrong reasons, i.e. that another process might be causing the overestimation of PBL moisture.

4 Case study 14 May 2004

The 14 May 2004 was another day with a typical summertime high-pressure situation and shallow convection was observed during the afternoon and evening over most of Germany.

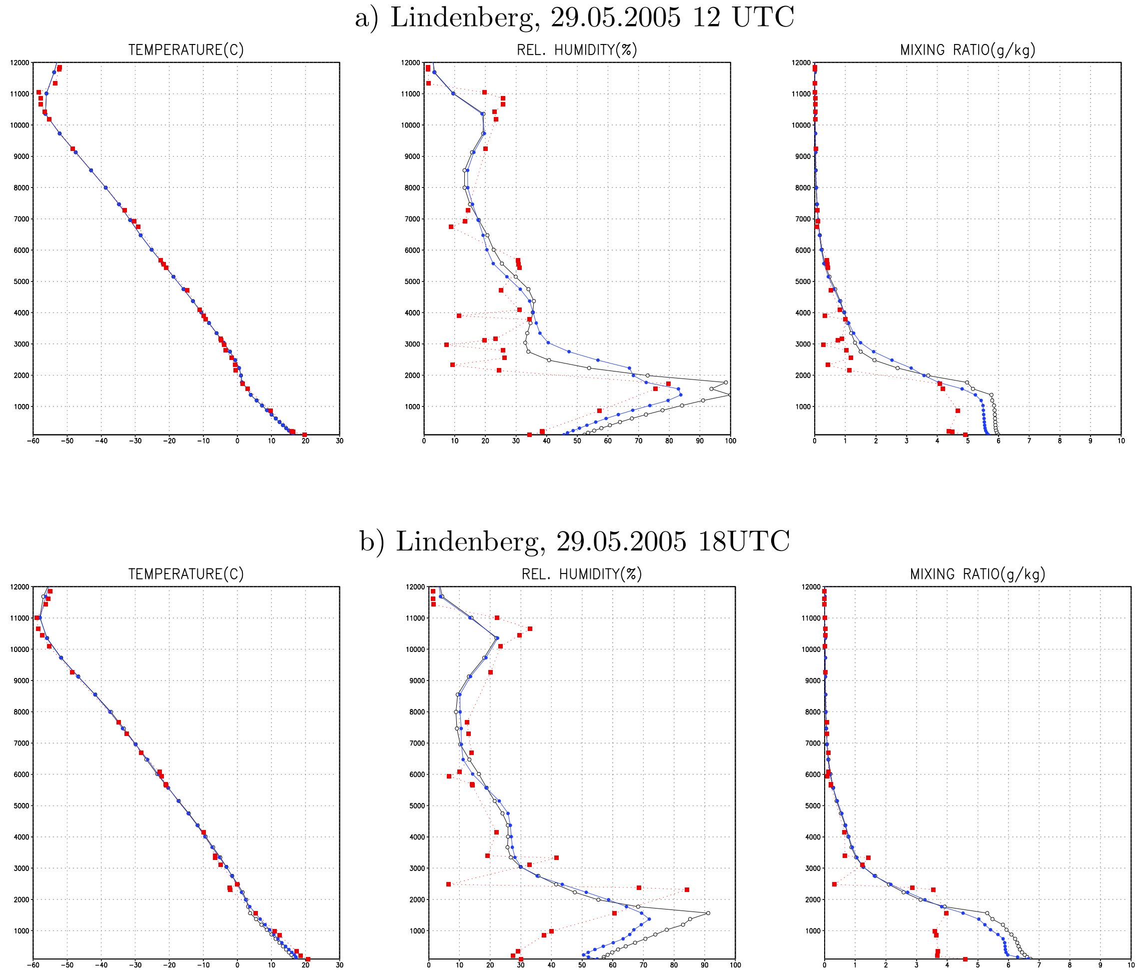

Figure 3: Vertical profiles of temperature, rel. humidity and water vapor mixing ratio at Lindenberg. Radiosonde measurements (red), LMK w/o shallow convection (black) and with shallow convection (blue)

Fig. 4 shows low-level cloud-cover at 18 UTC. In this case the difference between the two simulations is even more pronounced, without shallow convection the model predicts overcast conditions at 18 UTC while the simulation using the parameterization shows a greatly reduced cloud cover. The boundary problems without shallow convection scheme, especially in the SW-corner, result from the difference compared to the driving 7 km model that uses the full Tiedtke scheme and predicts a cloud cover quite similar to the high-resolution run with shallow convection scheme (see Doms and Förstner (2004) for a comparison of the 7 km vs 2.8 km model).

Fig. 5 shows the vertical profiles at Lindenberg. In this case the temperature profile is predicted reasonably well by both simulations, although the inversion at 2000 m AGL is more pronounced in the observations. The profiles of rel. humidity and vapor mixing ratio show that, in this case and at this specific grid point, the vertical transport of moisture by the shallow convection scheme leads to a growth of the PBL itself. By deposition of moisture right on top of the PBL the shallow convection increases the PBL height and also the maximum rel. humidity matching the observation much better than in the simulation without shallow convection scheme. Note that for this grid point the simulation with shallow convection predicts a higher cloud cover compared to the simulation without the parameterization.

Overall this case shows nicely that the LMK shallow convection scheme is necessary to ensure

a) without shallow conv. scheme b) with shallow conv. scheme

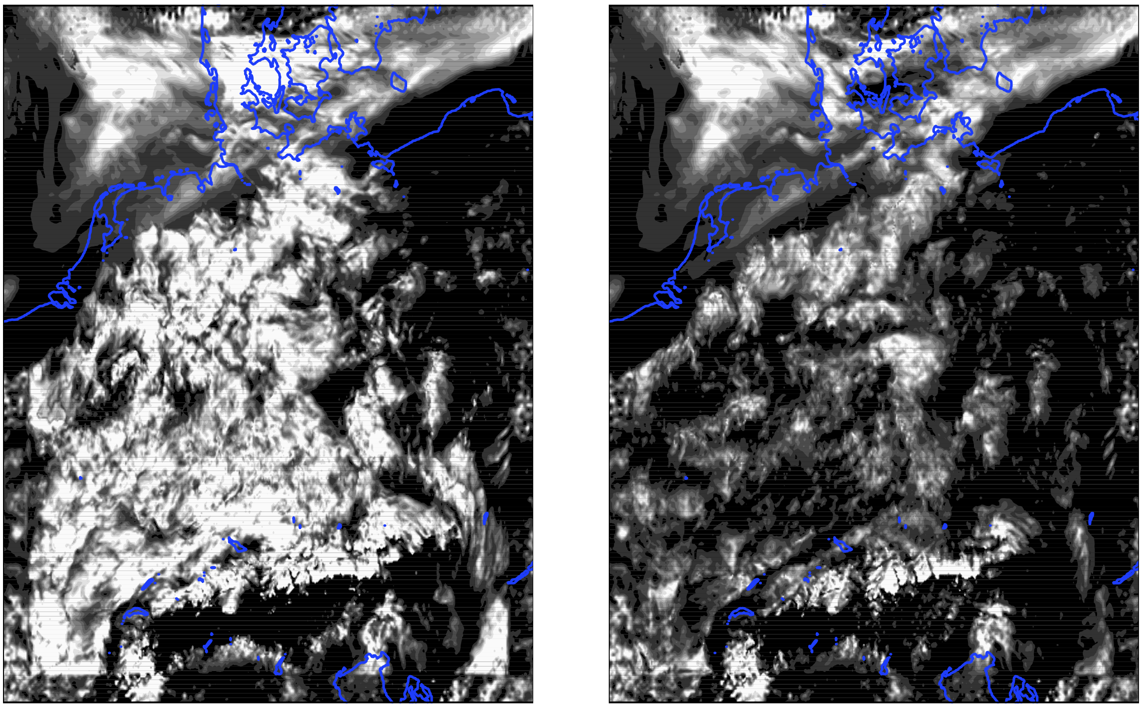

Figure 4: Simulated low-level cloud cover 14.05.2004 at 18 UTC in units of 1/8

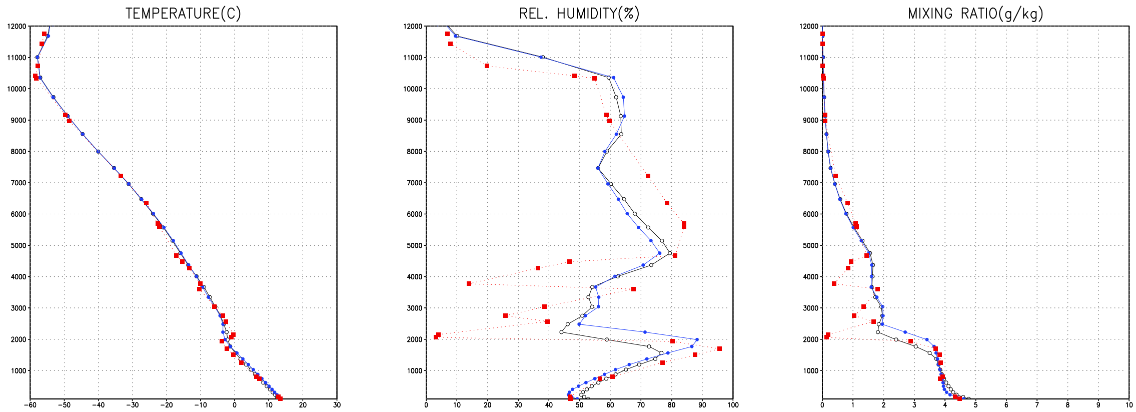

Figure 5: Vertical profiles of temperature, rel. humidity and water vapor mixing ratio at Lindenberg on 14 May 2004 18 UTC. Radiosonde measurements (red), LMK w/o shallow convection (black) and with shallow convection (blue).

consistency with the driving model and that the parameterized vertical transport of moisture may cause an increase of the PBL height at some grid points. Although the interaction of the shallow convection scheme and the PBL scheme has to be investigated more thoroughly, this PBL growth by shallow convection looks quite reasonable and might also be able to remove inversion layers in some cases, triggering resolved deep convection.

5 The w_*-closure

As already mentioned by Tiedtke (1989) and many others, shallow convection is mostly controlled by the sub-cloud layer turbulence. Therefore it is quite plausible to use a mass flux closure which is solely based on PBL turbulence parameters instead of the moisture convergence closure. In a high resolution NWP model this would implicitly assume that mesoscale convergence zones always trigger (resolved) deep convection.

For example, Neggers et al. (2004) suggest to use a mass flux closure proportional to the free convective velocity scale w_*:

$$M_u = a\, w_* = a \left(\frac{g z_b}{\theta_v^0} \overline{(w'\theta_v')_s} \right)^{\frac{1}{3}} \tag{1}$$

Here M_u ist the cloud base (specific) mass flux, z_b the PBL height and θ the potential temperature, i.e. $\overline{(w'\theta_v')_s}$ is the surface heat flux. Within the shallow convection scheme we assumed the z_b equals the cloud base height estimated by the parcel ascent.

Following Grant (2001) one may simply set $a = 0.03$ and this will be used in the following simulations, but note that Neggers et al. (2004) argue that a is in fact a function of the cloud fraction and should be parameterized using a statistical cloud scheme.

To compare the moisture convergence closure and the w_*-closure we have chosen the 20 May 2004. Fig. 6 shows low-level cloud cover at 6 UTC and 12 UTC. In the early morning hours we only see some differences over the Baltic sea where shallow convection might have been active in reality, too. Later on, the differences become larger and for this case the w_*-closure is even more efficient in reducing the low-level cloud cover. Fig. 7 shows time-height cross sections of measured radar reflectivity and simulated cloud cover at Lindenberg. The observations, which include also the estimated cloud base by a ceilometer, show an almost ideal development of a cloud-topped free convective boundary layer. Note that even a cloud radar cannot detect small, optically thin cumuli which were probably present during morning and noon, later on the clouds became thicker and even drizzle was formed in the late evening. The simulation using the moisture convergence closure reproduces the development of the PBL height very nicely and the amount of cloud cover, although not directly comparable to radar reflectivity, looks like a reasonable representation of the atmospheric conditions. Applying the w_*-closure leads to a more rapid development of the PBL height in the morning hours and more low-level cloud cover is observed earlier during the day. From this point of view, the moisture convergence closure seems to match the conditions somewhat better, although we have to keep in mind that this is only a single grid point.

6 Conclusions

Our sensitivity studies showed that using a simple shallow convection parameterization within the convection-resolving LMK improves directly the forecasts of low level cloud cover. Basically, this confirms the earlier results presented by Doms and Förstner (2004). The shallow convection is also necessary to ensure consistency with the driving larger-scale model which, at least at DWD, uses the Tiedtke parameterization.

The w_*-closure, although interesting, did not show any advantages in our case studies. Future work in this area will probably focus on the development of a generalized PBL scheme which includes shallow convection.

Further testing is needed for cases with (resolved) deep convection. Since the shallow convection scheme reduces the PBL moisture, it also reduces the convective available potential energy CAPE. Therefore we expect the deep convection to be slightly weaker in simulations using the shallow convection scheme.

a) q_v-convergence closure, 6 UTC b) w_*-closure, 6 UTC

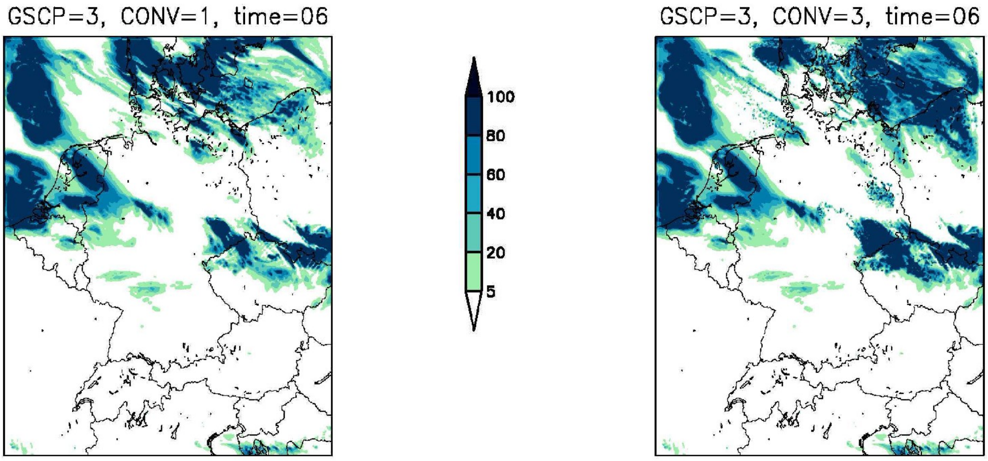

c) q_v-convergence closure, 12 UTC d) w_*-closure, 12 UTC

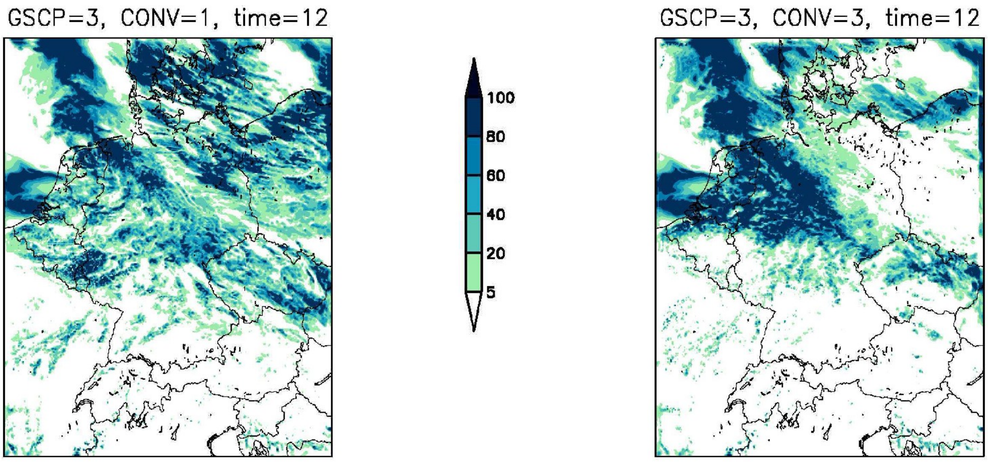

Figure 6: Simulated low-level cloud cover on 20.05.2004 in % (Note that the colors are reversed compared to Fig. 1)

References

Doms G. and J. Förstner, 2004: Development of a kilometer-scale NWP System: LMK. *COSMO Newsletter*, No. 4, pp. 159-167.

Grant, A., 2001: Cloud-base fluxes in the cumulus-capped boundary layer. *Quart. J. Roy. Met. Soc.*, 126, pp. 1913-1936.

Neggers, R., A. Siebesma, G. Lenderik and A. Holtslag, 2004: An Evaluation of Mass Flux Closures for Diurnal Cycles of Shallow Convection. *Mon. Wea. Rev.*, 132, pp. 2525-2538.

Tiedtke, M., 1989: A Comprehensive Mass Flux Scheme for Cumulus Parameterization in Large-Scale Models. *Mon. Wea. Rev.*, 117, pp. 1779-1800.

a) radar reflectivity and ceilometer cloud base

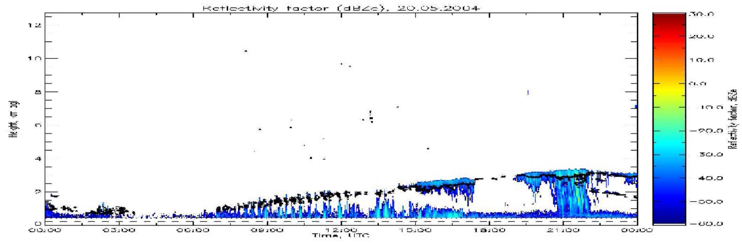

b) cloud fraction, q_v-convergence closure

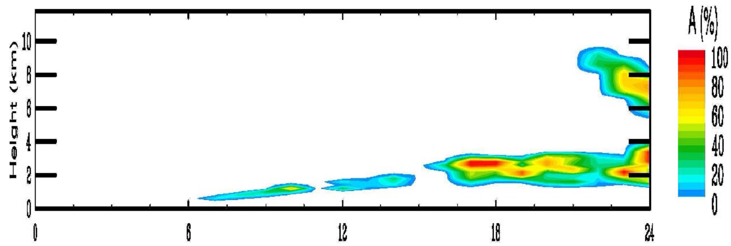

c) cloud fraction, w_* closure

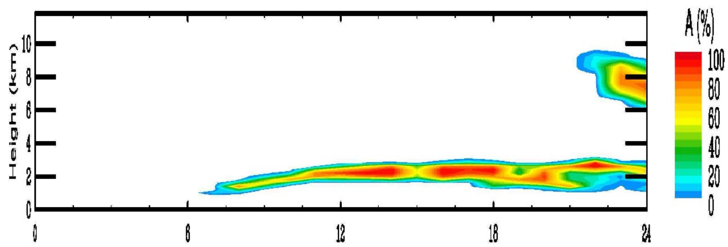

Figure 7: Time-Height cross sections of (a) observed radar reflectivity in dBZ (35 GHz cloud radar) and ceilometer cloud base height (black dots) as well as (b,c) simulated cloud cover in % at Lindenberg.